Histol Histopathol (2022) 37: 1019-1030

http://www.hh.um.es

Histology and Histopathology
From Cell Biology to Tissue Engineering

ORIGINAL ARTICLE **Open Access**

CircRNF220 plays a pathogenic role to facilitate cell progression of AML *in vitro* via sponging miR-330-5p to induce upregulation of SOX4

Zewen Zhang[1], Shujun Lin[2], Jun Yin[3], Wenjun Yu[1] and Chengwei Xu[4]

[1]Division of Hematology, The Second Affiliated Hospital of Shantou University Medical College, [2]Division of Nephrology, Shantou Central Hospital, [3]Department of Clinical Laboratory Medicine, The Second Affiliated Hospital of Shantou University Medical College and [4]Blood Purification Room, The Second Affiliated Hospital of Shantou University Medical College, Shantou, Guangdong, China

Summary. Background: Circular RNAs (circRNAs) are a specific family of non-coding RNAs (ncRNAs) with important function in disease progression. This research is performed to study circRNA Ring Finger Protein 220 (circRNF220) in acute myeloid leukemia (AML).

Methods: CircRNF220, microRNA-330-5p (miR-330-5p) and sex-determining region Y-related high-mobility group box 4 (SOX4) were measured via quantitative real-time polymerase chain reaction (qRT-PCR). 3-(4, 5-dimethylthiazol-2-y1)-2, 5- diphenyl tetrazolium bromide (MTT) and EdU assays were used to assess cell proliferation. Cell cycle and apoptosis were detected using flow cytometry. Cell invasion was determined by transwell assay. Glycolytic metabolism was assessed by glucose consumption and lactate production. The target interaction was implemented via dual-luciferase reporter and RNA pull-down assays. SOX4 protein detection was conducted by western blot.

Results: Expression detection identified that circRNF220 was overexpressed in AML. In vitro experiments showed that silence of circRNF220 promoted cell apoptosis but impeded proliferation, cell cycle progression, invasion and glycolytic metabolism in AML cells. Target analysis indicated that circRNF220 directly targeted miR-330-5p, and the effects of si-circRNF220 were abrogated by miR-330-5p inhibitor. Moreover, circRNF220 targeted miR-330-5p to increase the expression of SOX4 and SOX4 promoted cell progression of AML.

Conclusion: All these findings revealed that circRNF220 contributed to AML cell development in vitro via upregulating SOX4 expression by targeting miR-330-5p.

Corresponding Author: Zewen Zhang, Division of Hematology, The Second Affiliated Hospital of Shantou University Medical College, Dongxia Road North, Shantou, 515041, Guangdong, China. e-mail: zzw123778@126.com

DOI: 10.14670/HH-18-472

Key words: circRNF220, Acute myeloid leukemia, miR-330-5p, SOX4

Introduction

Acute myeloid leukemia (AML) is one of the most common hematologic diseases with aberrant proliferation and differentiation of immature myeloid blasts, eventually resulting in the loss of hematopoietic function (Thomas and Majeti, 2017). Increasing therapies have been developed in the medical research process of AML, such as cellular immunotherapy, chemotherapy, epigenetic therapy and FLT3 inhibitor treatment (Godwin et al., 2017; Bohl et al., 2018; Elshoury et al., 2019; Lee et al., 2019). AML is significantly associated with recurrent genetic abnormalities, mutations and monocytic differentiation (Jung et al., 2019). It is necessary to explore different molecular mechanisms of AML pathogenesis.

Noncoding circular RNAs (circRNAs) were first discovered in 1993 (Capel et al., 1993). CircRNAs have stable closed-loop structures generated by backsplicing of exons, and they are mainly localized in eukaryotic cytoplasm (Ebbesen et al., 2017; Salzman, 2016). Mounting evidence has demonstrated that circRNAs have cell-type differential expression and are closely relevant to the physiopathologic processes of multiple diseases (Chen and Huang, 2018), including AML (Jamal et al., 2019). Hsa_circ_0012152 is derived from

Abbreviations. circRNAs, Circular RNAs; ncRNAs, non-coding RNAs; circRNF220, circRNA Ring Finger Protein 220; AML, acute myeloid leukemia; miR-330-5p, microRNA-330-5p; SOX4, sex-determining region Y-related high-mobility group box 4; qRT-PCR, quantitative real-time polymerase chain reaction; MTT, 3-(4, 5-dimethylthiazol-2-y1)-2, 5-diphenyl tetrazolium bromide; WHO, World Health Organization; RNF220, Ring Finger Protein 220; miRNAs, MicroRNAs; 3'-UTRs, 3'-untranslated regions.

Ring Finger Protein 220 (RNF220) gene, and circRNA microarray has suggested that circRNF220 is upregulated in AML patients (Li et al., 2017). However, the function of circRNF220 in AML is not fully clear.

MicroRNAs (miRNAs) are small RNAs with ~22 nucleotides and can function as vital regulatory molecules in AML (Li and Guan, 2020). MiRNAs induce transcriptional and post-transcriptional regulation of genes by interacting with the 3'-untranslated regions (3'-UTRs) of target mRNAs (Vasudevan et al., 2007). MicroRNA-330-5p (miR-330-5p) was indicated to inhibit AML cell proliferation, migration and invasion (Lei et al., 2019) and TIM-3 was identified as a target gene of miR-330-5p in AML (Fooladinezhad et al., 2016). Sex-determining region Y-related high-mobility group box 4 (SOX4) is a crucial transcription factor mediating stemness, differentiation, and cancer development (Moreno, 2020). SOX4 functioned as an oncogene in C/EBPα mutant AML (H. Zhang et al., 2013) and miR-339-5p repressed proliferation of AML cells by downregulating SOX4 (X. Sun et al., 2018). The relation between miR-330-5p and SOX4 remains unclear.

In addition, circRNAs can regulate gene expression levels via acting as molecular sponges for miRNAs (Yin et al., 2019). The correlation of circRNF220 with miR-330-5p and SOX4 was disclosed in this study, providing a circRNF220-based pathological mechanism of AML *in vitro*.

Materials and methods

Ethical statement and clinical samples

All protocols were approved by the Ethical Review Committee of The Second Affiliated Hospital of Shantou University Medical College, and followed the ethical principles for biomedical research regarding human subjects in the Declaration of Helsinki. The written informed consent files were obtained from all individuals. Peripheral blood samples were collected from healthy volunteers (n=45) and AML patients (n=45) at The Second Affiliated Hospital of Shantou University Medical College. Subsequently, samples were centrifuged at 1200 rpm for 10 min and supernatant serums were saved in liquid nitrogen. The clinical parameters of AML patients are shown in Table 1. High and low RNA expression groups in patients were divided according to median values.

Cell culture and transfection

Human bone marrow cell line HS-5 was acquired from American Type Culture Collection (ATCC, Manassas, VA, USA) and cultured in Dulbecco's modified eagle medium (DMEM; Gibco, Carlsbad, CA, USA). AML cell lines (THP-1, MV4-11, KG-1, HL-60, and AML2) were purchased from COBIOER Biosciences Co., Ltd (Nanjing, China) and maintained in

Table 1. Relationship between clinicopathological parameters of AML patients and expression of circRNF20 or miR-330-5p or SOX4.

Characteristics	circRNF20 expression			miR-330-5p expression			SOX4 expression		
	Low (N=22)	High (N=23)	P-value	Low (N=22)	High (N=23)	P-value	Low (N=22)	High (N=23)	P-value
Median level (range)	3.74856 (2.4857-4.8574)	5.9587 (4.870-7.5241)	<0.0001 1	0.28769 (0.0985-0.3608)	0.43847 (0.3614-0.6532)	<0.0001 01	1.87527 (1.2635-2.2812)	2.90234 (2.4085-4.0691)	<0.0001 1
Gender			0.8615			0.668			0.3015
Male	13	13		12	14		11	15	
Female	9	10		10	9		11	8	
Age, year			0.2989			0.672			0.8482
>20	12	16		13	15		14	14	
≤20	10	7		9	8		8	9	
Median WBC (range), ($\times 10^9$/L)	11.23 (1-603.7)	20.5 (0.8-612)	0.2466	10.56 (0.6-524.5)	21 (1-612)	0.149	13.2 (1-610.4)	20.4 (0.6-612)	0.4049
Bone marrow Blasts (range), %	51.3 (2-97)	54 (3-91)	0.9716	54.3 (2-90)	56.4 (2-97)	0.982	52.4 (2-95)	55.7 (2-97)	0.9334
Peripheral blood Blasts (range), %	22 (0-88)	34 (0-91)	0.3333	24 (0-90)	26 (0-91)	0.931	21 (0-87)	33 (0-91)	0.3175
FAB classification			0.0883			0.051			0.0207
M1-M4	16	11		10	17		17	10	
M5-M7	6	12		12	6		5	13	
Clinical Risk†			0.7149			0.905			0.733
Favorable	5	4		4	5		5	4	
Intermediate	7	10		9	8		9	8	
Poor	10	9		9	10		8	11	
Gene mutation			0.5981			0.673			0.5981
CEBPA (+/-)	3/19	2/21		2/20	3/20		3/19	2/21	

AML, Acute myeloid leukemia; WBC, White blood cells; FAB, French-American British.

Roswell Park Memorial Institute-1640 (RPMI-1640; Gibco). Fetal bovine serum (FBS; 10%, Gibco) and antibiotic solution (100 unit/mL penicillin and 100 μg/mL streptomycin; Gibco) were complemented into the basic media for cell growth and depollution. Cells were cultured in a humidified incubator with 5% CO_2 at 37°C.

Lipofectamine 3000 reagent (Invitrogen, Carlsbad, CA, USA) was used for transfection of oligonucleotides in THP-1 and HL-60 cells, following the manufacturer's explanatory memorandum. Small interfering RNA (siRNA) targeting circRNF220 and SOX4 (si-circRNF220 and si-SOX4), miR-330-5p mimic (miR-330-5p), miR-330-5p inhibitor (anti-miR-330-5p) and matched negative control oligonucleotides (si-NC, miR-NC and anti-miR-NC) were synthesized from RIBOBIO (Guangzhou, China).

RNA isolation and the quantitative real-time polymerase chain reaction (qRT-PCR)

Total RNA was isolated from serum samples and cell lines using RNAiso Plus (Takara, Shiga, Japan). The complementary DNA (cDNA) was obtained by reverse transcription of 1 μg RNA via PrimeScript™ RT reagent Kit (Takara) and amplified by TB Green® Fast qPCR Mix (Takara) on Applied Biosystems 7300 Real-Time PCR System (Applied Biosystems, Foster City, CA, USA). In addition, circRNF220 localization was assessed by qRT-PCR after the separation of nuclear and cytoplasmic fractions through PARIS™ Kit (Invitrogen). All used primers were synthesized by Sangon (Shanghai, China): circRNF220 (sense: 5'-TGGCCTCATTTC TGATCGGG-3', antisense: 5'-GCGTTACGCAAGAAG CAGTC-3'), RNF220 mRNA (sense: 5'-CACGGCAA GTCTTAGGAGGG-3', antisense: 5'-CCGGTGTAAGT CCATCGGAG-3'), miR-330-5p (sense: 5'-GCCGAG TCTCTGGGCCTGTGT-3', antisense: 5'-CTCGTATC CAGTGCAGGGTC-3'), SOX4 (sense: 5'-CTTGA CATGATTAGCTGGCATGATT-3', antisense: 5'-CCTG TGCAATATGCCGTGTAGA-3'), 18S rRNA (sense: 5'-GCAATTATTCCCCATGAACG-3', antisense: 5'-GGGACTTAATCAACGCAAGC-3'), and U6 (sense: 5'-CTCGCTTCGGCAGCACA-3', antisense: 5'-AACGCTTCACGAATTTGCGT-3'). It was specially noted that circRNF220 primer was designed by targeting circular sequence of circRNF220. 18S rRNA acted as the reference gene for circRNA and mRNA, as well as U6 for miRNA. Data analysis was performed by $2^{-\Delta\Delta C}t$ method and -ΔΔCt was expressed as: $(\Delta Ct_{\text{experimental group target gene}} - Ct_{\text{experimental group reference gene}}) - (\Delta C_{\text{tcontrol group target gene}} - Ct_{\text{control group reference gene}})$.

Stability analysis

The stability of circRNF220 was analyzed after cell treatment with 2 mg/mL Actinomycin D (Millipore, Billerica, MA, USA) for the indicated time (0 h, 8 h, 16 h and 24 h) or RNA treatment with 3 U/μg Ribonuclease R (RNase R; Epicentre Technologies, Madison, WI, USA) for 30 min at 37°C. Then, qRT-PCR was used for detecting the levels of circRNF220 and RNF220 mRNA.

3-(4, 5-dimethylthiazol-2-y1)-2, 5-diphenyl tetrazolium bromide (MTT) assay

1×10^4/well THP-1 and HL-60 cells at logarithmic growth phase were seeded into 96-well plates. After cell transfection for different times (0 h, 24 h, 48 h, 72 h), each well was added with 10 μL 12 mM MTT stock solution (Invitrogen) and viable cells restored to formazan crystal. After incubation for 4 h, cell supernatant was removed and formazan was dissolved with 100 μL/well SDS-HCI solution (Invitrogen), followed by reading the absorbance at 570 nm via a Multiskan™ FC microplate reader (Thermo Fisher Scientific, Waltham, MA, USA).

EdU assay

Cell proliferation ability was assessed by EdU Cell Proliferation Kit (Sangon). Briefly, THP-1 and HL-60 cells were incubated with 100 μL EdU detection solution for 30 min. Cell nuclei were stained with 300 μL diamidine phenylindole (DAPI; Sangon) for 20 min. Cells were washed with 300 μL PBS twice, then cell images were taken by fluorescence microscope (Olympus, Tokyo, Japan) and EdU-positive (EdU+DAPI) cells were counted.

Flow cytometry

For cell cycle, cells were stained with Propidium Iodide (PI) using Cell Cycle Assay Kit (Dojindo Molecular Technologies, Kumamoto, Japan) following the manufacturer's instruction. Cell proportion was measured by a flow cytometer (BD Biosciences, San Diego, CA, USA). For cell apoptosis, cells were stained with Annexin V-fluorescein isothiocyanate (Annexin V-FITC) and PI using Annexin V Apoptosis Detection Kit (Dojindo Molecular Technologies). Annexin V (+)/PI (-) and Annexin V (+)/PI (+) labeled cells were counted as the apoptotic cells on BD Accuri C6 flow cytometer (BD Biosciences) using BD Accuri C6 system (32-bit) software (BD Biosciences).

Invasion assay

The top chamber of transwell chamber (Corning Inc., Corning, NY, USA) was coated with matrigel (Corning Inc.), and added with 1×10^5 cells in serum-free RPMI-1640 medium. Then 0% FBS+RPMI-1640 medium was pipetted into the bottom chamber. 24 h later, cells passed into the bottom chamber were fastened by 4% Paraformaldehyde Fix Solution and stained with crystal violet (Sangon). The invaded cells were imaged by an inverted microscope (Olympus) at 100× magnification, and counted under 5 visual fields.

Assessment of glycolytic metabolism

Glucose detection was performed by Glucose Assay Kit-WST® (Dojindo Molecular Technologies). 1×10^6 cells were seeded into 6-well plates overnight and transfected for 48 h, then 100 μL supernatants were diluted with ultrapure water. The 96-well plates were added with 50 μL samples or glucose standard solution, and incubated with 50 μL Working solution at 37°C for 30 min. Lactate production was determined by Lactate Assay Kit-WST® (Dojindo Molecular Technologies). 20 μL cell supernatants were diluted with ultrapure water. Then 96-well plates were incubated with 20 μL samples or lactate standard solution and added with 80 μL Working solution at 37°C for 30 min. The glucose consumption and lactate production were assessed by assaying absorbance at 450 nm via a microplate reader (Thermo Fisher Scientific).

Dual-luciferase reporter assay

Circinteractome (https://circinteractome.nia.nih.gov/) and starbase (http://starbase.sysu.edu.cn/index.php) were used for prediction of binding sites between circRNF220 or SOX4 and miR-330-5p. The wild-type (WT) sequences of circRNF220 and SOX4 3'UTR were inserted into the luciferase-expressing vector pGL3-control (Promega, Madison, WI, USA) to produce circRNF220-WT and SOX4 3'UTR-WT. The predicted binding sites of miR-330-5p in circRNF220 or SOX4 3'UTR were mutated and the mutant-type (MUT) sequences were also cloned into pGL3-control vector to construct circRNF220-MUT and SOX4 3'UTR-MUT. THP-1 and HL-60 cells were co-transfected with constructed vector and miR-330-5p or miR-NC. After 48 h-incubation, cell supernatant was harvested for the measurement of luciferase activity by dual-luciferase reporter assay system (Promega). The relative luciferase activity was expressed as the ratio of firefly to renilla.

Biotinylated RNA pull-down assay

THP-1 and HL-60 cells were transfected with biotinylated-miR-330-5p (Bio-miR-330-5p), Bio-miR-330-5p-MUT or Bio-miR-NC. Cell lysates were mixed with C-1 magnetic beads (Life Technologies, Carlsbad, CA, USA) overnight at 4°C. After RNA extraction from magnetic beads, qRT-PCR was used for quantification of circRNF220. In addition, cell lysates were incubated with magnetic beads covered with Bio-circRNF220, Bio-circRNF220-MUT or Bio-NC. The miR-330-5p enrichment was determined by qRT-PCR analysis.

Western blot

After cell transfection for 48 h, RIPA lysis buffer (high intensity) was used for protein extraction. Protein concentration was examined by total protein assay kit (with standard: BCA method), and 40 μg proteins were separated on electrophoresis precast gels (10%, 10 well) in SDS-PAGE electrophoresis buffer. Protein transfer to PVDF membranes, prevention of non-specific binding, incubation of the primary antibodies/secondary antibody and ECL detection were performed by Western Blot Detection Kit. The primary antibody targeting SOX4 (ab90696, 1:1000) or glyceraldehyde-phosphate dehydrogenase (GAPDH; ab37168, 1:3000) and the secondary antibody (ab205718, 1:5000) were bought from Abcam (Cambridge, UK). The detection reagents were all purchased from Nanjing Jiancheng Bioengineering Institute (Nanjing, China). GAPDH was used as an internal control and SOX4 protein expression was analyzed by ImageLab software version 4.1 (Bio-Rad, Hercules, CA, USA). The original protein images of three repetitions are shown in Supplementary file 1.

Statistical analysis

All experiments were independently carried out with three times and three parallels. The final data were revealed as mean ± standard deviation (SD). SPSS 24.0 (IBM Corp., Armonk, NY, USA) and Graphpad Prism 7 (GraphPad Inc., La Jolla, CA, USA) were applied for statistical analysis. The linear relationship was analyzed via Pearson's correlation coefficient. The pairwise difference was evaluated by Student's t-test and comparisons among multiple groups were conducted using one-way analysis of variance (ANOVA) followed by Tukey's test. P value less than 0.05 represented a significant difference.

Results

CircRNF220 was identified as a highly expressed circRNA in AML

CircRNA array analysis in GSE94591 showed that circRNF220 (hsa_circ_0012152) was one of the top 5 up-regulated circRNAs in AML patients in contrast with healthy controls (Fig. 1A). CircRNF220 is localized in the chr1:44877652-44878394 with mature splicing length of 742 bp (Fig. 1B). To detect the expression of circRNF220 in AML, we designed specific primers targeting the circular sequence of circRNF220. The qRT-PCR data confirmed the up-regulation of circRNF220 in AML serums (Fig. 1C) and cells (THP-1, MV4-11, KG-1, HL-60, and AML2) (Fig. 1D) compared with healthy control serums and HS-5 cells. The half-life of circRNF220 was longer than RNF220 after the transcription inhibition of Actinomycin D (Fig. 1E-F) and circRNF220 was more resistant to RNase R than RNF220 (Fig. 1G-H). Additionally, circRNF220 was localized in the cytoplasm using 18S rRNA (cytoplasmic gene) and U6 (small nuclear RNA) as control groups (Fig. 1I-J). CircRNA220 was an upregulated circRNA in AML samples and cells.

Silencing circRNF220 inhibited AML cell growth, cell cycle progression, invasion, and glycolytic metabolism in vitro

CircRNF220 siRNA was transfected into THP-1 and HL-60 cells. The qRT-PCR analysis showed that circRNF220 was knocked down by approximately 65% and linear RNF220 level was not changed by si-circRNF220 (Fig. 2A). MTT assay exhibited that silence of circRNF220 induced proliferation inhibition of THP-1 and HL-60 cells (Fig. 2B). EdU assay showed that EdU-positive cells were reduced in si-circRNF220 group relative to si-NC group, further affirming that circRNF220 promoted AML cell proliferation (Fig. 2C). Flow cytometry revealed that knockdown of circRNF220 retarded cell cycle transition from G0/G1 phase to S phase (Fig. 2D) but enhanced cell apoptotic rate (Fig. 2E). Transwell assay indicated that invaded cell number was inhibited by siRNA of circRNF220 (Fig. 2F). Then, glucose consumption (Fig. 2G) and lactate production (Fig. 2H) were displayed to be decreased by silencing circRNF220 in THP-1 and HL-60 cells. These results collectively confirmed that silencing circRNF220 repressed AML cell progression *in vitro*.

CircRNF220 directly targeted miR-330-5p

Online circinteractome was used for target prediction of circRNF220, and circRNF220 sequence contained a binding region of miR-330-5p (Fig. 3A). In THP-1 and HL-60 cells, miR-330-5p mimic induced significant overexpression of miR-330-5p by more than 5-fold (Fig. 3B). Upregulation of miR-330-5p resulted in a suppressive influence on the relative luciferase activity of circRNF220-WT luciferase plasmid but no conspicuous effect was observed on the mutant circRNF220-MUT (Fig. 3C-D). Biotin-coupled RNA pull-down assay revealed that circRNF220 was pulled down by miR-330-5p in THP-1 and HL-60 cells (Fig. 3E), as well as the pull-down of miR-330-5p by circRNF220 (Fig. 3F). Through the comparison with healthy control serums and control HS-5 cells, miR-330-5p was found to be downregulated in AML serums and cells (THP-1 and HL-60) (Fig. 3G-H). Pearson's correlation coefficient analysis reflected a negative relationship (r=-0.7676, P<0.0001) between circRNF220

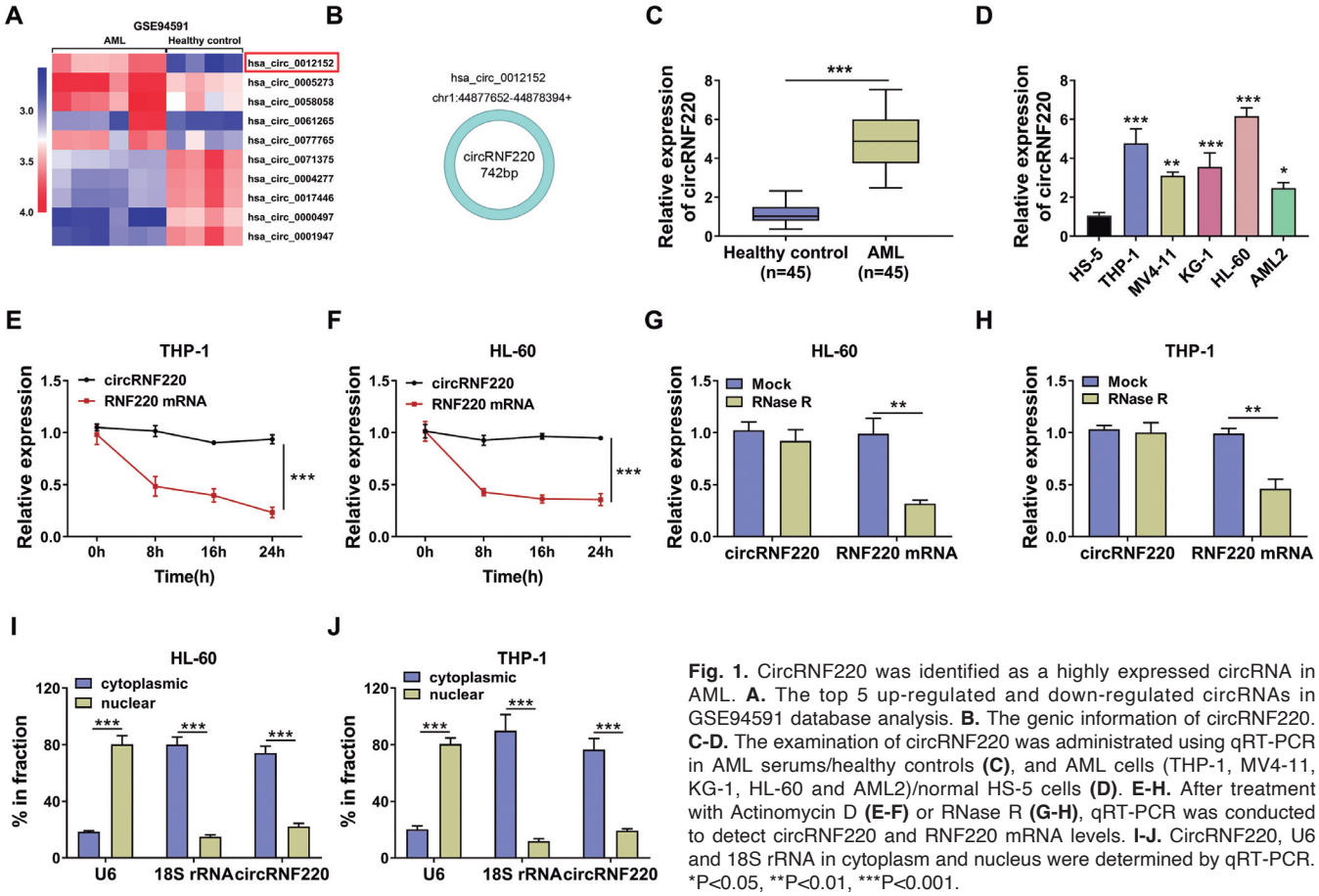

Fig. 1. CircRNF220 was identified as a highly expressed circRNA in AML. **A.** The top 5 up-regulated and down-regulated circRNAs in GSE94591 database analysis. **B.** The genic information of circRNF220. **C-D.** The examination of circRNF220 was administrated using qRT-PCR in AML serums/healthy controls **(C)**, and AML cells (THP-1, MV4-11, KG-1, HL-60 and AML2)/normal HS-5 cells **(D)**. **E-H.** After treatment with Actinomycin D **(E-F)** or RNase R **(G-H)**, qRT-PCR was conducted to detect circRNF220 and RNF220 mRNA levels. **I-J.** CircRNF220, U6 and 18S rRNA in cytoplasm and nucleus were determined by qRT-PCR. *P<0.05, **P<0.01, ***P<0.001.

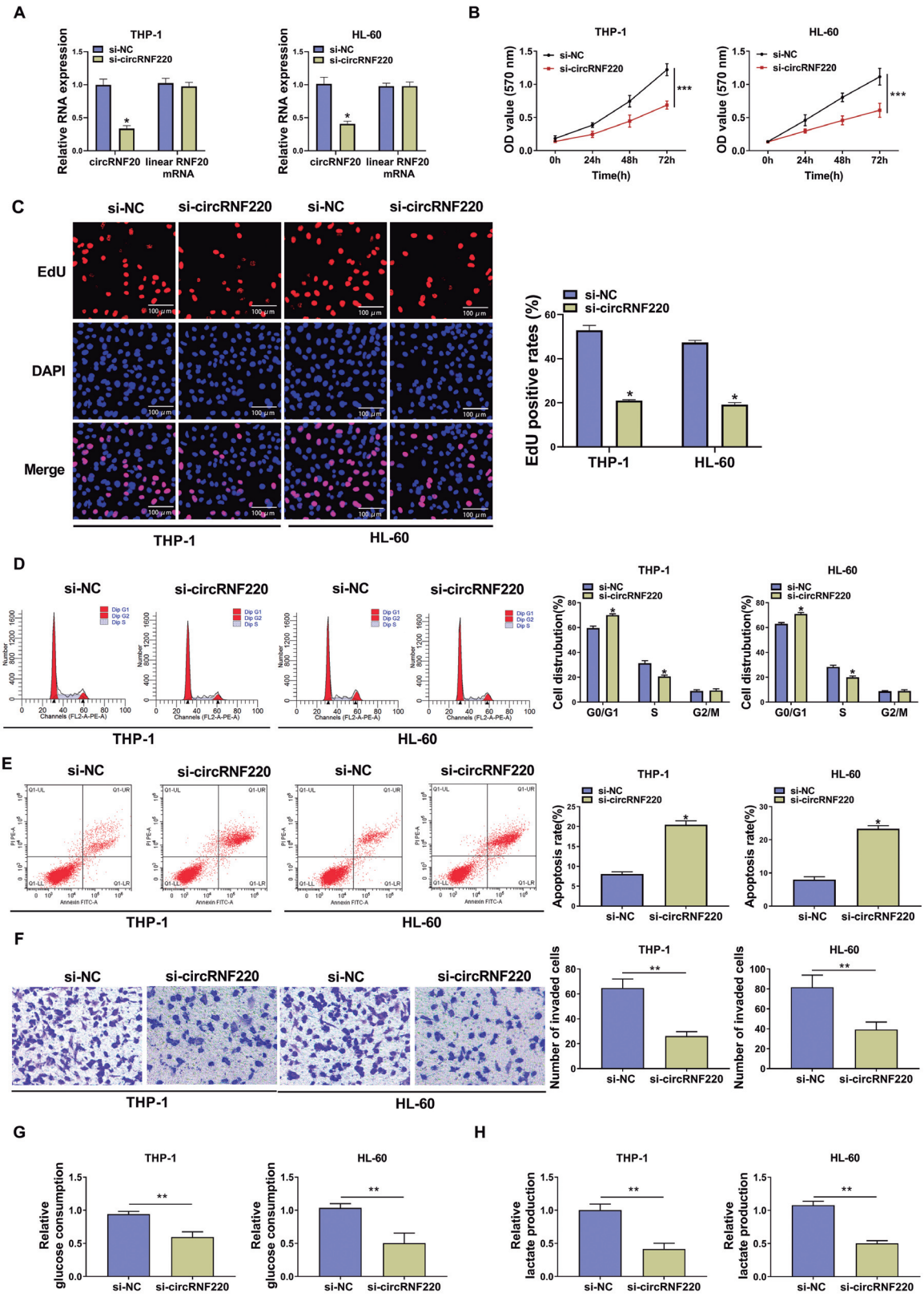

Fig. 2. Silencing circRNF220 inhibited AML cell growth, cell cycle progression, invasion, and glycolytic metabolism in vitro. **A.** CircRNF220 and RNF220 levels were measured by qRT-PCR in THP-1 and HL-60 cells transfected with si-NC or si-circRNF220.**B-C.** MTT assay **(B)** and EdU assay **(C)** were performed for the analysis of cell proliferation. **D-F.** Flow cytometry was conducted to measure cell cycle progression **(D)** and cell apoptosis **(E)**. **F.** Transwell assay was used for evaluating cell invasion. **G-H.** Glucose consumption and lactate production were assayed for the assessment of glycolytic process. *P<0.05, **P<0.01, ***P<0.001.

and miR-330-5p in 45 AML serums (Fig. 3I). Besides, miR-330-5p level upregulation was detected in THP-1 and HL-60 cells after silence of circRNF220 (Fig. 3J) while miR-330-5p overexpression did not affect the expression of circRNF220 (Fig. 3K). Thus, circRNF220 directly targeted miR-330-5p.

MiR-330-5p inhibitor neutralized the impairment of si-circRNF220 on AML cell development

Given the target relation between circRNF220 and miR-220-5p, reverted experiments were performed to study the circRNF220/miR-330-5p axis in AML cellular processes. The data from qRT-PCR assay showed that miR-330-5p upregulation induced by si-circRNF220 was attenuated by anti-miR-330-5p, exhibiting the effective transfection of anti-miR-330-5p in THP-1 and HL-60 cells (Fig. 4A). As a result of miR-330-5p inhibition, si-circRNF220-mediated cell proliferation inhibition (Fig. 4B-C), cell cycle retardation (Fig. 4D), cell apoptosis promotion (Fig. 4E) and invasion repression (Fig. 4F) were all counterbalanced. Also, si-circRNF220-inhibited glucose consumption and lactate production were partly restored by miR-330-5p inhibitor (Fig. 4G-H). The above evidences confirmed that circRNF220 regulated AML cell development via targeting miR-330-5p.

CircRNF220 knockdown downregulated SOX4 expression by increasing miR-330-5p

Target genes of miR-330-5p were predicted by starbase software and SOX4 was shown to have binding sites with miR-330-5p (Fig. 5A). Dual-luciferase reporter results indicated the luciferase inhibition of SOX4 3'UTR-WT plasmid rather than SOX4 3'UTR-MUT after miR-330-5p was upregulated in THP-1 and HL-60 cells (Fig. 5B-C). The results of qRT-PCR and western blot exhibited that miR-330-5p overexpression reduced SOX4 mRNA and protein levels (Fig. 5D-E). Knockdown of circRNF220 evoked mRNA and protein

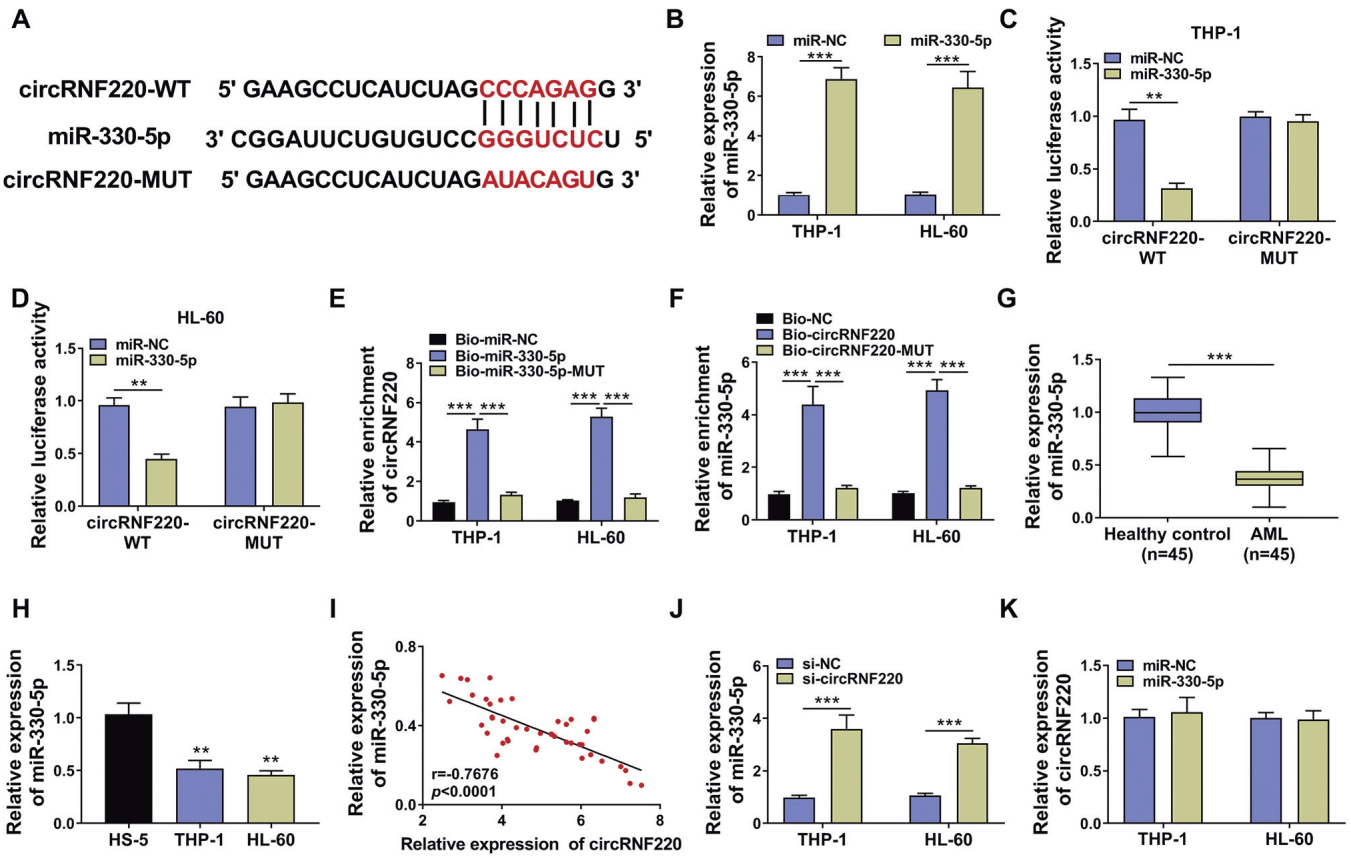

Fig. 3. CircRNF220 directly targeted miR-330-5p. **A.** The binding of circRNF220 and miR-330-5p in sites was presented by circinteractome. **B.** The miR-330-5p level was analyzed by qRT-PCR after transfection of miR-330-5p or miR-NC. **C-D.** Dual-luciferase reporter assay was applied to study the binding between circRNF220 and miR-330-5p. **E-F.** RNA pull-down assay was implemented for proving the capture of circRNF220 **(E)** and miR-330-5p **(F)** by miR-330-5p and circRNF220, respectively. **G-H.** The expression pattern of miR-330-5p was analyzed via qRT-PCR in AML serums **(G)** and cells **(H)**. **I.** The relationship analysis between circRNF220 and miR-330-5p was carried out using Pearson's correlation coefficient. **J-K.** qRT-PCR was used to measure the effect of si-circRNF220 on miR-330-5p level **(J)**, and miR-330-5p on circRNF220 level **(K)**. **P<0.01, ***P<0.001.

downregulation of SOX4, while anti-miR-330-5p transfection antagonized this inhibition (Fig. 5F-G). TCGA database (http://gepia.cancer-pku.cn/detail.php?gene=SOX4) showed that SOX4 was evidently increased in AML patients (n=173) compared with normal controls (n=70) (Fig. 5H). Also, SOX4 mRNA and protein levels were higher in AML serums than healthy control serums (Fig. 5I-J). In addition, SOX4 protein level was upregulated in THP-1 and HL-60 cells relative to HS-5 cells (Fig. 5K). A negative association (r=-0.6605, P<0.0001) between miR-330-5p and SOX4 expression was detected (Fig. 5L), while circRNF220 was positively related to SOX4 (r=0.6413, P<0.0001) in AML serums (Fig. 5M). SOX4 was a target of miR-330-5p, and circRNF220 affected SOX4 expression via targeting miR-330-5p.

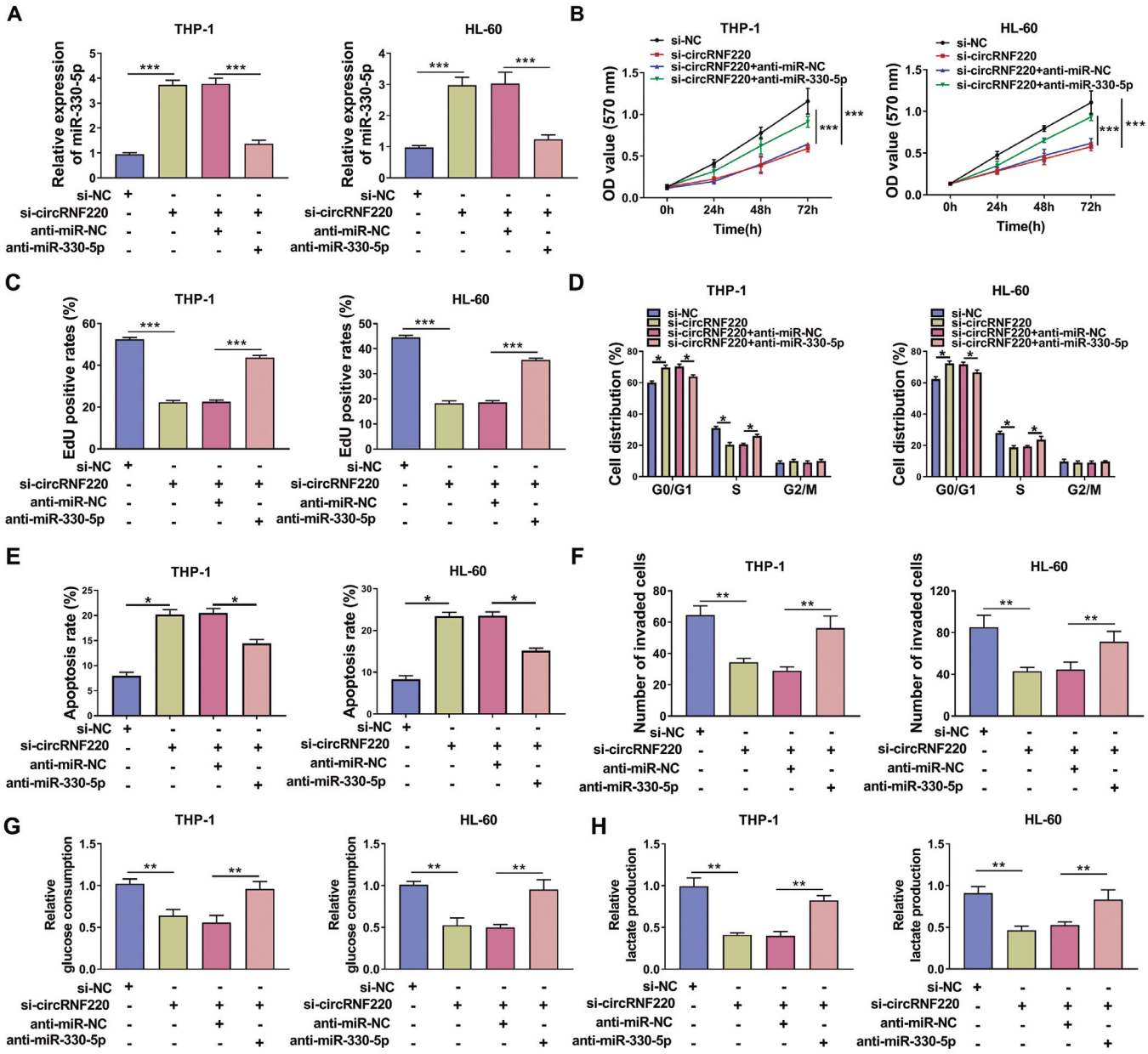

Fig. 4. MiR-330-5p inhibitor neutralized the impairment of si-circRNF220 on AML development. **A.** After transfection of si-NC, si-circRNF220, si-circRNF220+anti-miR-NC or si-circRNF220+anti-miR-330-5p, the analysis of miR-330-5p level was performed through qRT-PCR. **B-C.** The determination of cell proliferation was performed by MTT assay **(B)** and EdU assay **(C)**. **D-F.** The detection of cell cycle **(D)** and apoptosis **(E)** was performed by flow cytometry. **F.** The measurement of cell invasion was conducted by transwell assay. **G-H.** Glycolytic metabolism was evaluated by the consumption of glucose and the production of lactate. *P<0.05, **P<0.01, ***P<0.001.

SOX4 served as an oncogene in AML

Furthermore, the role of SOX4 in AML was analyzed. As the qRT-PCR and western blot data in Fig. 6A-B, SOX4 mRNA and protein levels were inhibited after siRNA transfection. Downregulation of si-SOX4 has led to the inhibitory effects on cell proliferation (Fig. 6C-D) and cell cycle progression (Fig. 6E) but a promoting effect on apoptosis (Fig. 6F) in THP-1 and HL-60 cells. Cell invasive ability was also suppressed after the expression knockdown of SOX4 (Fig. 6G). Moreover, glucose consumption (Fig. 6H) and lactate production (Fig. 6I) were decreased in si-SOX4-transfected cells in contrast with the si-NC-transfected cells. Taken together, SOX4 was a pathogenic gene in AML and the regulation of circRNF220/miR-330-5p in AML cell progression was achieved by acting on SOX4.

Discussion

AML is a heterogeneous disease with high morbidity and mortality especially in older patients, and ncRNAs are found to have essential regulatory function in AML (Y. Liu et al., 2019). In this study, the biological regulation and molecular mechanism of circRNF220 in in AML cell progression were clarified.

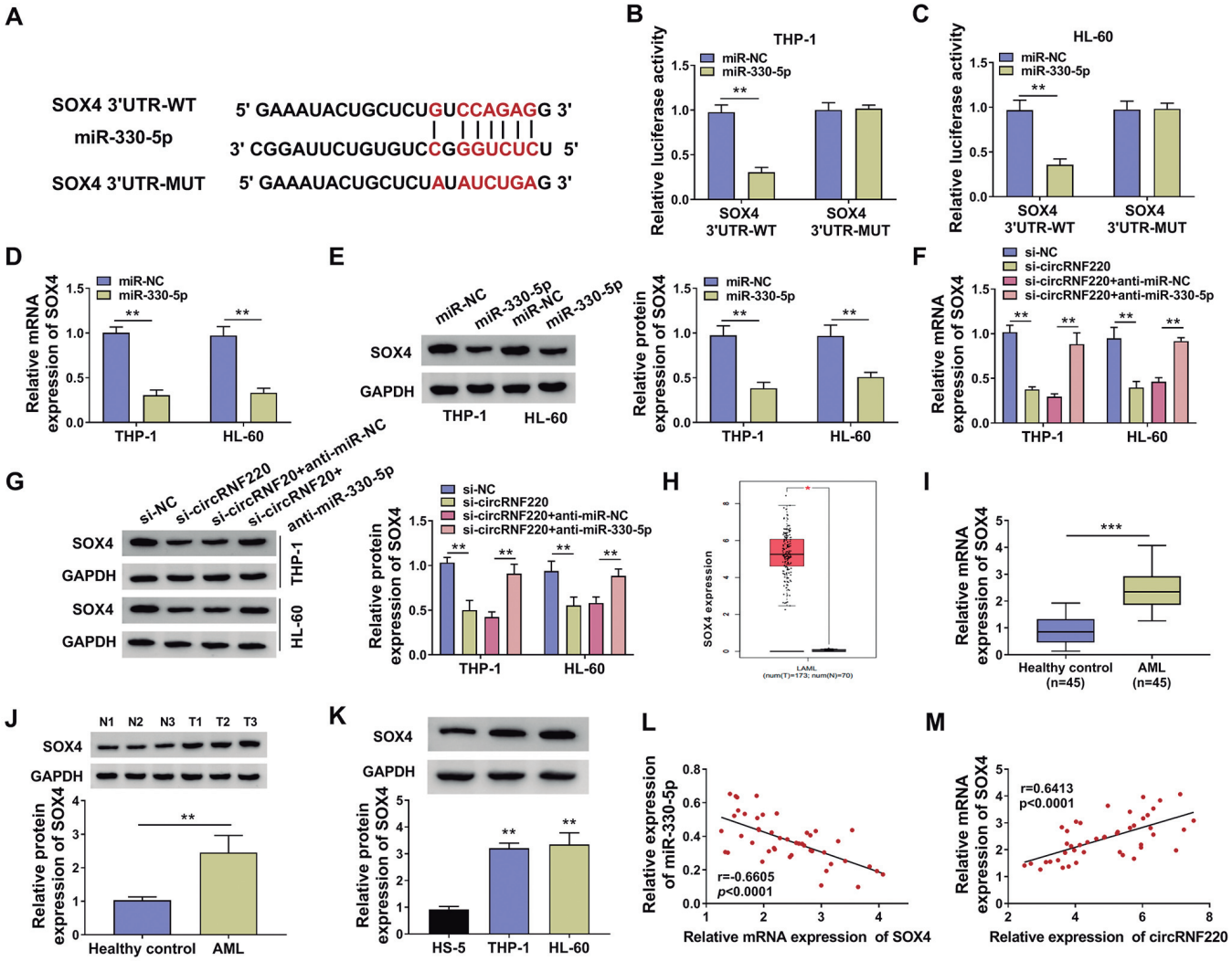

Fig. 5. CircRNF220 knockdown downregulated SOX4 expression by increasing miR-330-5p. **A.** The starbase was used as a prediction software for showing the binding sites between miR-330-5p and SOX4 3'UTR. **B-C.** The combination of miR-330-5p and SOX4 was analyzed by performing dual-luciferase reporter assay. **D-G.** qRT-PCR and western blot were employed to detect the effects of miR-330-5p or miR-NC **(D-E)**, si-circRNF220/miR-330-5p axis **(F-G)** on SOX4 expression. (H) The SOX4 expression in AML and normal serums in TCGA database. **I-J.** The measurement of SOX4 mRNA and protein expression in AML serums and healthy controls was conducted by qRT-PCR and western blot. **K.** Western blot was adopted for assaying the protein level of SOX4 in HS-5, THP-1 and HL-60 cells. **L-M.** Pearson's correlation coefficient was used for linear analysis between miR-330-5p and SOX4 **(L)**, as well as circRNF220 and SOX4 **(M)**. **P<0.01, ***P<0.001.

Our expression detection affirmed that circRNF220 was abnormally up-regulated in AML samples and cells. CircRNAs with binding junction of 5' and 3' ends have higher stability than linear transcripts with the termination of 5' caps or 3' tails (Shi et al., 2008). Herein, circRNF220 was resistant to Actinomycin D treatment and exonucleolytic degradation compared to linear inform RNF220. The high stability identified the existence of circRNF220 in AML cells.

Many studies have illuminated the biological function of circRNAs in various types of diseases. For example, circRNA F-circEA-4a promoted migration and invasion of non-small cell lung cancer cells (Tan et al., 2018). Circ_15698 upregulation exacerbated the accumulation of extracellular matrix in diabetic nephropathy (Hu et al., 2019). Overexpression of

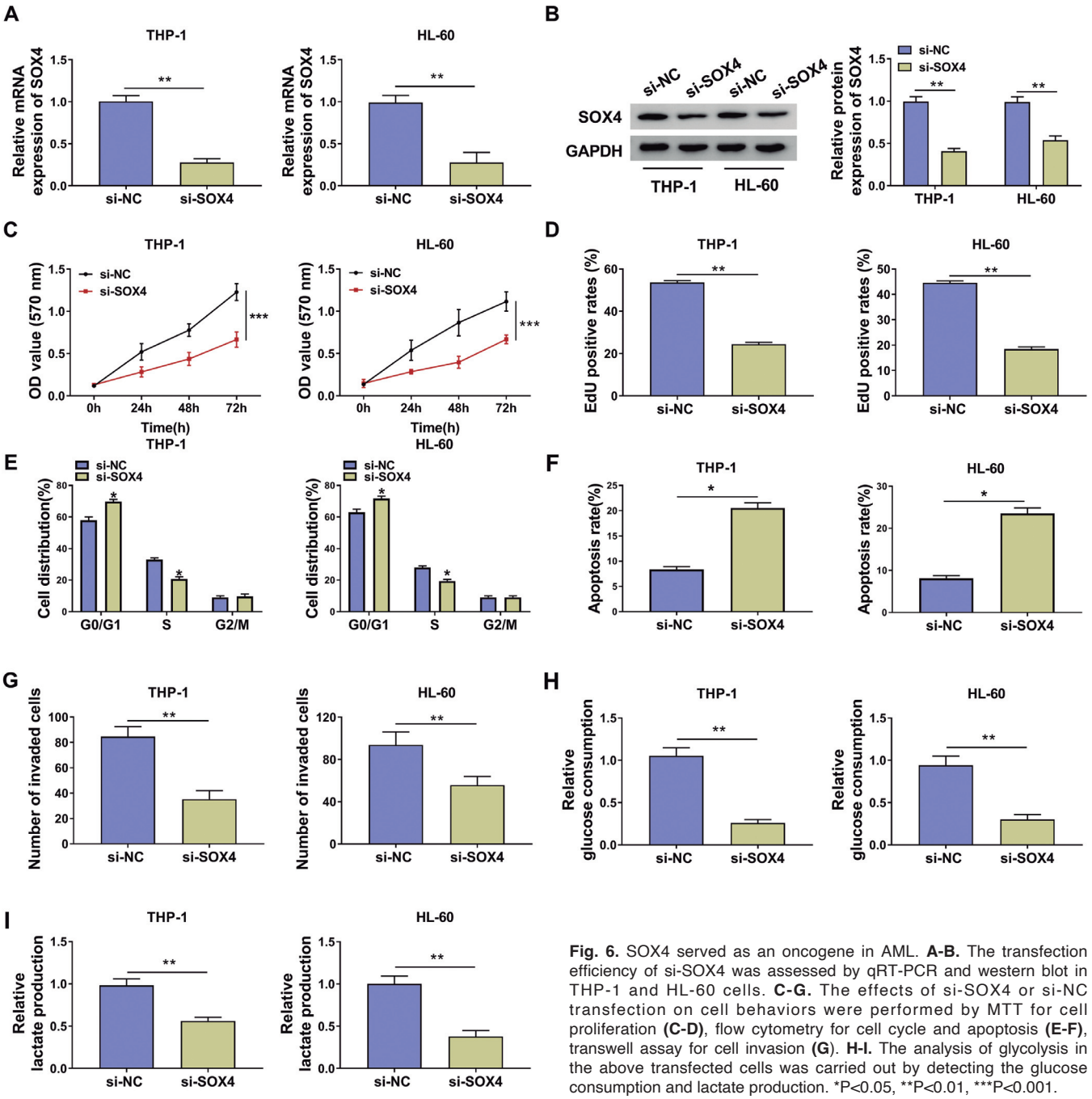

Fig. 6. SOX4 served as an oncogene in AML. **A-B.** The transfection efficiency of si-SOX4 was assessed by qRT-PCR and western blot in THP-1 and HL-60 cells. **C-G.** The effects of si-SOX4 or si-NC transfection on cell behaviors were performed by MTT for cell proliferation **(C-D)**, flow cytometry for cell cycle and apoptosis **(E-F)**, transwell assay for cell invasion **(G)**. **H-I.** The analysis of glycolysis in the above transfected cells was carried out by detecting the glucose consumption and lactate production. *P<0.05, **P<0.01, ***P<0.001.

circHECTD1 was correlated to disease severity, inflammatory response and recurrent possibility in acute ischemic stroke (Peng et al., 2019). In recent years, circRNAs have been increasingly researched in hematological malignancies (Mei et al., 2019). For AML, circMYBL2 was reported to accelerate the progression in FLT3-ITD AML (Sun et al., 2019) and circANAPC7 overexpression was involved in the pathogenesis of AML (Chen et al., 2018). Liu et al. found that circRNF220 downregulation reduced proliferation and enhanced apoptosis in AML cells (Liu et al., 2021). Consistent with this study, our results indicated that silencing circRNF220 repressed AML cell proliferation and induced cell apoptosis. In addition, we have detected the effects of circRNF220 on other biological behaviors. Cell cycle progression and cell invasion were also inhibited after knockdown of circRNF220. Cancer progression is associated with various metabolic pathways (Hiller and Metallo, 2013). Glycolytic metabolism is a significant pathway to support cancer cell proliferation and development (Ganapathy-Kanniappan and Geschwind, 2013). Our data demonstrated that glucose consumption and lactate production were suppressed by circRNF220 level inhibition, implying that circRNF220 might block the glycolytic process in AML cell progression.

The sponge roles of circRNAs have been uncovered for different miRNAs, such as circ-cTFRC/miR-107 axis in bladder cancer (Su et al., 2019), circ_104433/miR-497-5p axis in gastric cancer (Wei et al., 2020), circ_100290/miR-203 axis in AML (Fan et al., 2018).Circ_0009910 was revealed to regulate AML cell growth by sponging miR-20a-5p (Ping et al., 2019). Our analysis manifested that circRNF220 acted as a miR-330-5p sponge and circRNF220 affected AML cell progression via targeting miR-330-5p.

SOX4 is correlated to poor prognosis of AML patients (Lu et al., 2017), and can regulate oncogenic signals in acute lymphoblastic leukemia (Ramezani-Rad et al., 2013). Herein, our data demonstrated that SOX4 knockdown inhibited the malignant behaviors of AML cells. In addition, SOX4 was identified as a target of miR-330-5p and circRNF220 induced the positive regulation of SOX4 via sponging miR-330-5p. CircRNF220 has been shown to upregulate MYSM1 and IER2 levels by sequestering miR-30a (Liu et al., 2021), and we have elucidated another miRNA/mRNA axis for circRNF220 in AML. A variety of reports have suggested the involvement of circRNA/miRNA/mRNA axis in AML. Wu et al. declared that circDLEU2 enhanced AML cell proliferation and blocked cell apoptosis through PRKACB upregulation via downregulating miR-496 (Wu et al., 2018). Zhang et al. suggested that circ_0000370 contributed to AML progression via miR-1299-mediated expression elevation of S100A7A (Zhang et al., 2020). Thus, circRNF220 function in AML cell progression was achieved by upregulating SOX4 via targeting miR-330-5p.

In conclusion, circRNF220 up-regulated SOX4 to promote the leukemogenesis of AML by acting as a sponge of miR-330-5p. CircRNF220/miR-330-5p/SOX4 axis is a novel molecular pathogenesis for AML.

Acknowledgements. None.

Disclosure of interest. The authors declare that they have no financial conflicts of interest.

References

Bohl S.R., Bullinger L. and Rucker F.G. (2018). Epigenetic therapy: azacytidine and decitabine in acute myeloid leukemia. Expert Rev. Hematol. 11, 361-371.

Capel B., Swain A., Nicolis S., Hacker A., Walter M., Koopman P., Goodfellow P. and Lovell-Badge R. (1993). Circular transcripts of the testis-determining gene Sry in adult mouse testis. Cell 73, 1019-1030.

Chen B. and Huang S. (2018). Circular RNA: An emerging non-coding RNA as a regulator and biomarker in cancer. Cancer Lett. 418, 41-50.

Chen H., Liu T., Liu J., Feng Y., Wang B., Wang J., Bai J., Zhao W., Shen Y., Wang X., Yang J., Ji Y., He A. and Yang Y. (2018). Circ-ANAPC7 is upregulated in acute myeloid leukemia and appears to target the MiR-181 family. Cell Physiol. Biochem. 47, 1998-2007.

Ebbesen K.K., Hansen T.B. and Kjems J. (2017). Insights into circular RNA biology. RNA Biol. 14, 1035-1045.

Elshoury A., Przespolewski A., Baron J. and Wang E.S. (2019). Advancing treatment of acute myeloid leukemia: the future of FLT3 inhibitors. Expert Rev. Anticancer Ther. 19, 273-286.

Fan H., Li Y., Liu C., Liu Y., Bai J. and Li W. (2018). Circular RNA-100290 promotes cell proliferation and inhibits apoptosis in acute myeloid leukemia cells via sponging miR-203. Biochem. Biophys. Res. Commun. 507, 178-184.

Fooladinezhad H., Khanahmad H., Ganjalikhani-Hakemi M. and Doosti A. (2016). Negative regulation of TIM-3 expression in AML cell line (HL-60) using miR-330-5p. Br. J. Biomed. Sci. 73, 129-133.

Ganapathy-Kanniappan S. and Geschwind J.F. (2013). Tumor glycolysis as a target for cancer therapy: progress and prospects. Mol. Cancer 12, 152.

Godwin C.D., Gale R.P. and Walter R.B. (2017). Gemtuzumab ozogamicin in acute myeloid leukemia. Leukemia 31, 1855-1868.

Hiller K. and Metallo C.M. (2013). Profiling metabolic networks to study cancer metabolism. Curr. Opin. Biotechnol. 24, 60-68.

Hu W., Han Q., Zhao L. and Wang L. (2019). Circular RNA circRNA_15698 aggravates the extracellular matrix of diabetic nephropathy mesangial cells via miR-185/TGF-beta1. J. Cell Physiol. 234, 1469-1476.

Jamal M., Song T., Chen B., Faisal M., Hong Z., Xie T., Wu Y., Pan S., Yin Q., Shao L. and Zhang Q. (2019). Recent progress on circular RNA research in acute myeloid leukemia. Front. Oncol. 9, 1108.

Jung J., Cho B.S., Kim H.J., Han E., Jang W., Han K., Lee J.W., Chung N.G., Cho B., Kim M. and Kim Y. (2019). Reclassification of acute myeloid leukemia according to the 2016 WHO classification. Ann. Lab. Med. 39, 311-316.

Lee J.B., Chen B., Vasic D., Law A.D. and Zhang L. (2019). Cellular immunotherapy for acute myeloid leukemia: How specific should it be? Blood Rev. 35, 18-31.

Lei B., He A., Chen Y., Cao X., Zhang P., Liu J., Ma X., Qian L. and

Zhang W. (2019). Long non-coding RNA RPPH1 promotes the proliferation, invasion and migration of human acute myeloid leukemia cells through down-regulating miR-330-5p expression. EXCLI J. 18, 824-837.

Li W., Zhong C., Jiao J., Li P., Cui B., Ji C. and Ma D. (2017). Characterization of hsa_circ_0004277 as a new biomarker for acute myeloid leukemia via circular RNA profile and bioinformatics analysis. Int. J. Mol Sci. 18, 597.

Li M., Cui X. and Guan H. (2020). MicroRNAs: pivotal regulators in acute myeloid leukemia. Ann. Hematol. 99, 399-412.

Liu Y., Cheng Z., Pang Y., Cui L., Qian T., Quan L., Zhao H., Shi J., Ke X. and Fu L. (2019). Role of microRNAs, circRNAs and long non-coding RNAs in acute myeloid leukemia. J. Hematol. Oncol. 12, 51.

Liu X., Liu X., Cai M., Luo A., He Y., Liu S., Zhang X., Yang X., Xu L. and Jiang H. (2021). CircRNF220, not its linear cognate gene RNF220, regulates cell growth and is associated with relapse in pediatric acute myeloid leukemia. Mol. Cancer. 20, 139.

Lu J.W., Hsieh M.S., Hou H.A., Chen C.Y., Tien H.F. and Lin L.I. (2017). Overexpression of SOX4 correlates with poor prognosis of acute myeloid leukemia and is leukemogenic in zebrafish. Blood Cancer J. 7, e593.

Mei M., Wang Y., Li Z. and Zhang M. (2019). Role of circular RNA in hematological malignancies. Oncol. Lett. 18, 4385-4392.

Moreno C.S. (2020). SOX4: The unappreciated oncogene. Semin. Cancer Biol. 67, 57-64.

Peng X., Jing P., Chen J. and Xu L. (2019). The role of circular RNA HECTD1 expression in disease risk, disease severity, inflammation, and recurrence of acute ischemic stroke. J. Clin. Lab. Anal. 33, e22954.

Ping L., Jian-Jun C., Chu-Shu L., Guang-Hua L. and Ming Z. (2019). Silencing of circ_0009910 inhibits acute myeloid leukemia cell growth through increasing miR-20a-5p. Blood Cells Mol. Dis. 75, 41-47.

Ramezani-Rad P., Geng H., Hurtz C., Chan L.N., Chen Z., Jumaa H., Melnick A., Paietta E., Carroll W.L., Willman C.L., Lefebvre V. and Muschen M. (2013). SOX4 enables oncogenic survival signals in acute lymphoblastic leukemia. Blood 121, 148-155.

Salzman J. (2016). Circular RNA expression: Its potential regulation and function. Trends Genet. 32, 309-316.

Shi Z., Yang W.Z., Lin-Chao S., Chak K.F. and Yuan H.S. (2008). Crystal structure of *Escherichia coli* PNPase: central channel residues are involved in processive RNA degradation. RNA 14, 2361-2371.

Su H., Tao T., Yang Z., Kang X., Zhang X., Kang D., Wu S. and Li C. (2019). Circular RNA cTFRC acts as the sponge of MicroRNA-107 to promote bladder carcinoma progression. Mol. Cancer 18, 27.

Sun X., Liu H., Li T. and Qin L. (2018). MicroRNA3395p inhibits cell proliferation of acute myeloid leukaemia by directly targeting SOX4. Mol. Med. Rep. 18, 5261-5269.

Sun Y.M., Wang W.T., Zeng Z.C., Chen T.Q., Han C., Pan Q., Huang W., Fang K., Sun L.Y., Zhou Y.F., Luo X.Q., Luo C., Du X. and Chen Y.Q. (2019). circMYBL2, a circRNA from MYBL2, regulates FLT3 translation by recruiting PTBP1 to promote FLT3-ITD AML progression. Blood 134, 1533-1546.

Tan S., Sun D., Pu W., Gou Q., Guo C., Gong Y., Li J., Wei Y.Q., Liu L., Zhao Y. and Peng Y. (2018). Circular RNA F-circEA-2a derived from EML4-ALK fusion gene promotes cell migration and invasion in non-small cell lung cancer. Mol. Cancer 17, 138.

Thomas D. and Majeti R. (2017). Biology and relevance of human acute myeloid leukemia stem cells. Blood. 129, 1577-1585.

Vasudevan S., Tong Y. and Steitz J.A. (2007). Switching from repression to activation: microRNAs can up-regulate translation. Science 318, 1931-1934.

Wei W., Mo X., Yan L., Huang M., Yang Y., Jin Q., Zhong H., Cao W., Wu K., Wu L., Li Z., Wang T., Qin Y. and Chen J. (2020). Circular RNA profiling reveals that circRNA_104433 regulates cell growth by targeting miR-497-5p in gastric cancer. Cancer Manag. Res. 12, 15-30.

Wu D.M., Wen X., Han X.R., Wang S., Wang Y.J., Shen M., Fan S.H., Zhang Z.F., Shan Q., Li M.Q., Hu B., Chen G.Q., Lu J. and Zheng Y.L. (2018). Role of circular RNA DLEU2 in human acute myeloid leukemia. Mol. Cell Biol. 38, e00259-18.

Yin Y., Long J., He Q., Li Y., Liao Y., He P. and Zhu W. (2019). Emerging roles of circRNA in formation and progression of cancer. J. Cancer 10, 5015-5021.

Zhang H., Alberich-Jorda M., Amabile G., Yang H., Staber P.B., Di Ruscio A., Welner R.S., Ebralidze A., Zhang J., Levantini E., Lefebvre V., Valk P.J., Delwel R., Hoogenkamp M., Nerlov C., Cammenga J., Saez B., Scadden D.T., Bonifer C., Ye M. and Tenen D.G. (2013). Sox4 is a key oncogenic target in C/EBPalpha mutant acute myeloid leukemia. Cancer Cell 24, 575-588.

Zhang L., Bu Z., Shen J., Shang L., Chen Y. and Wang Y. (2020). A novel circular RNA (hsa_circ_0000370) increases cell viability and inhibits apoptosis of FLT3-ITD-positive acute myeloid leukemia cells by regulating miR-1299 and S100A7A. Biomed. Pharmacother. 122, 109619.

Accepted May 25, 2022